Voltage Sag Planning of Distributed Generation System with Special Connection Transformers Using Particle Swarm Optimization Considering Sensitive Loads

Ying-Pin Chang[1] , Lieh-Dai Yang[2]

[1]Department of Electrical and Information Engineering, Nan Kai University of Technology
[2]Department of Industrial Management, Nan Kai University of Technology

通訊作者：張英彬
聯絡地址：南投縣草屯鎮中正路 568 號
電子郵件：cyp@nkut.edu.tw
投稿日期：2013 年 8 月
接受日期：2013 年 11 月

Abstract

This paper investigates the voltage sag planning of distributed generation (DG) system for three-phase to two-phase connection transformers with Scott and Le Blanc. The particle swarm optimization (PSO) method was used to determine the design values. This analysis considers the sensitive loads and over-current relays coordination. The model composed of node admittance matrix for voltage sag calculation was investigated to obtain the system sag severity after single or two-phase faults. The analytical equations were useful in the mathematical method of optimal planning. The PSO was then used to obtain suitable transformer impedances and the values of relay time multiplier parameters. The search for the global optimal solution was applied to the voltage sag problems in tests on the power systems with Scott, and Le Blanc, respectively, connection transformers were chosen to reveal the effectiveness of this method. Finally, the study results showed that the voltage sag severity could be improved by tuning the transformer impedances and relay settings.

Keywords: Distributed generation (DG)**,** voltage sag, power quality, sensitive loads, particle swarm optimization method, special connection transformers.

1. Introduction

The renewable energy sources are growing interest in environmental issues; the primary sources most often used in application are wind, solar power, heat power, fuel cells and hydro power. In order to achieve the sustainable power system reliability combined with DG, some grid operators already require voltage sag study. Therefore, the voltage sag has received much attention in the post of distributed generation systems. It was added into distribution system may cause some variety problems, such as frequency, harmonics, and voltage sag. Thus, in different standards some limits are recommended for interconnecting condition such as IEEE standard 1547^{TM}. Recently, DG applications have been used to improve the power quality of the utility grid and reliability of distribution system. Milanovic Ali and Aung (2007) presented the effect of DG units on the voltage sag of interruptions and their mitigating influence on the severity of voltage sag were investigated by Macke, Bollen and Belmans (2004), and Bollen (1999). However, the DG units can reduce the consequences of voltage sags, industrial customers would be more inclined to install DG units. The positive impact during voltage sags of balance and unbalance fault even in special connection transformers to the medium to high voltage levels is well-known.

The proliferation of different nonlinear loads in electrical systems has resulted in the voltage sag. It is one of the power quality degradation indexes and a useful measure of interruptions and fault events. Some momentary faults would cause voltage sag during the transient period until protective relays are activated, and the circuit breakers clean the faults. The voltage sag study shows that the system voltage can be reduced to 10% or 90% of the normal value in a period of a few cycles by IEEE Standard 446 (1995), IEEE Standard 1100-2005 (2006), and IEEE Standard 1159 (1995). The study is comprised of three parts, the drop in the voltage (△V) such as Das (1990) and Mahdianpoor, Hooshmand, and Ataei (2011), the duration (△t) such as Yalcinkaya, Bollen,and Crossley (1998), and the possible number such as Wang, Chen and Lie. (2005). While △V is determined by the system impedances and fault types, △t is determined by the protective relays and the circuit breakers action time. One of the limitations is given by the Information Technology Industry Council (ITIC), as plotted in Figure 1 by Gomez and Morcos (2002), Kyei, Ayanar, Heydt and Thallam (2001), Gomez and Lee, Albu and Heydt (2004), Heydt and Jewell (1998). Additionally, the Semiconductor Equipment and Materials International (SEMI) have also developed a SEMI curve to define the ability of semiconductor devices and equipment during voltage sag. Another voltage of the limitation is give by the IEEE standard 1547 as Table 1.

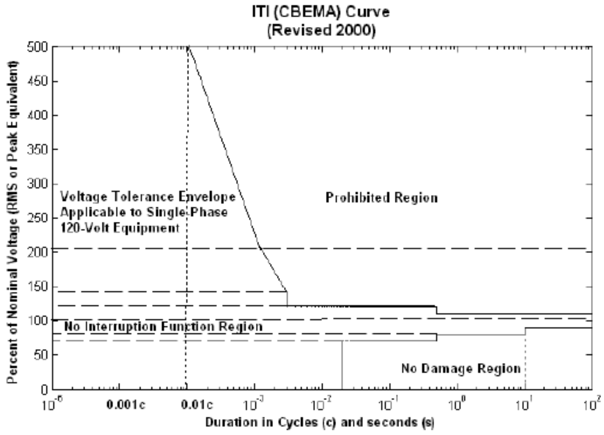

Fig. 1 ITI power acceptability curve.

Table 1 Interconnection system response to abnormal voltages of IEEE standard 1547^{TM}

Voltage rang (% of the base voltage)	Clearing time (s)
V ＜ 50％	0.16
50％ ≦ V ＜ 88％	2.00
88％ ≦ V ≦ 110％	Interconnection
110％ ＜ V ＜ 120％	1.00
V ≧ 120％	0.16

Some special electrical systems usually require strong single-phase power sources. To reduce the voltage unbalance disturbances to three-phase sources, some special connection transformers are used, such as Scott, and Le Blanc connection schemes. These schemes have been employed in railway electrification systems. The power quality study issues in railway electrification systems include influences of traction loads on three-phase utility systems. For example, Chen and Kuo (1995) propose a network model which was proposed for investigating the unbalance effects and a short circuit current study was conducted by Huang, Kuo, Chan, Lu, and Huang (2001).

However, the voltage sag study of DG power system with special connection transformers have not been addressed enough. It is still needed to investigate the equivalent transformers models for three-phase power flow, the network models for unbalance effects, and the short circuit current model for fault analysis. This paper reveals suitable calculation method of short circuit voltages and currents in a power system with special connection transformers. The node admittance matrix models are used. Ko, Chang and Wu (2009), Kumar, Kalyan and Mishra

(2011), He, Xu, and Huang (2009), Chang (2010), Deihimi and Momeni (2012) presented the voltage sag planning using the PSO method, which is a direct and parallel search method that involves accelerating and migrant operations to prevent falling into local optimal solutions. This optimization method enables determining system equipment parameters over a wide range. The transformer impedances and protective relay time multiple settings are variables. Calculation values are compared with the voltage sag acceptability curve (VSAC) of ITI and IEEE standard 1547 as plotted in Figure 2. The convergent characteristics of this approach are also compared with that of the neural network. Finally, the voltage sag severity of DG power system with the special connection transformer can be greatly improved using the proposed method.

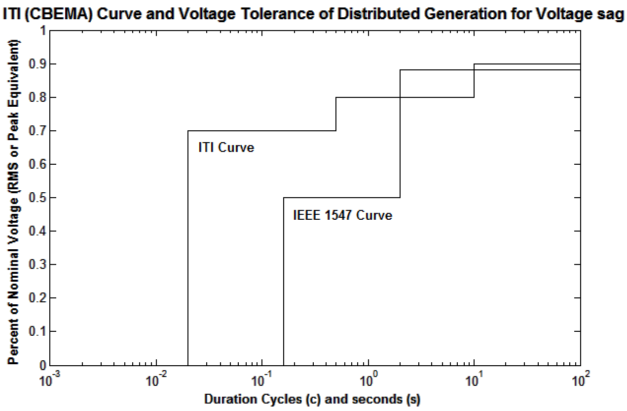

Fig.2 ITI (CBEMA) curve and IEEE standard 1547™ of voltage sag.

2. Methods

The three-phase to two-phase of analytical models for special connection transformers are required in the optimal design procedure. There are two connection schemes, Scott and Le Blanc. The models are developed with winding connections and phase coordinates, considering the copper loss and phase-angle displacement between the primary and secondary voltages.

2.1 The three-phase to two-phase special connection transformers

Scott connection comprised of two different turn ratio transformers. The main transform (phase M) has a center-tapped winding on the primary side, and a single winding on the secondary side. The teaser transformer (phase T) is a single-phase transformer. The phase difference between M and T is 90°. In addition to, Le Blanc connection scheme of the primary windings are the same as those of a general three-phase transformer in the delta connection. The secondary side consists of five windings, which are separated into two phases.

2.2 Short circuit fault calculation

The per-unit values are used in the calculation. Figure 3 reveals DG power system with a three-phase to two-phase transformer. The source is a balanced three-phase Y connection 161-kV power system. The distributed generation source is a balanced three-phase Y connection 690-V. There are four voltage levels including 161-kV, 69-kV, 27.5-kV, and 0.69-kV.

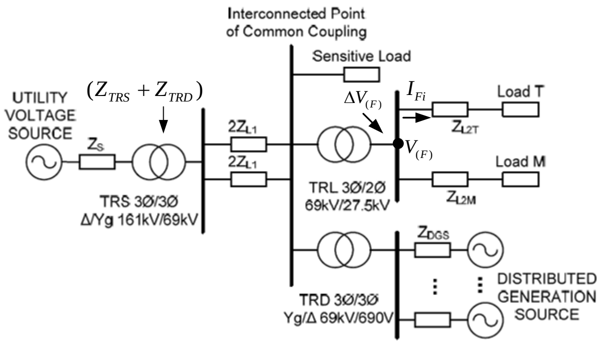

Fig. 3 Distribution network with railway loads, sensitive loads and DGs.

The equivalent model for the short circuit calculation of DG power system with special connection transformers is given in Figure 4. Let the source voltages be

$$\begin{bmatrix} V_{SA} \\ V_{SB} \\ V_{SC} \end{bmatrix} = \frac{V}{\sqrt{3}} \begin{bmatrix} \angle 0^\circ \\ \angle -120^\circ \\ \angle 120^\circ \end{bmatrix} \tag{1}$$

The equivalent injected currents are then expressed as

$$\begin{bmatrix} I_{SA} \\ I_{SB} \\ I_{SC} \end{bmatrix} = \frac{1}{Z_{TRS}+Z_{TRD}} \begin{bmatrix} V_{SA} \\ V_{SB} \\ V_{SC} \end{bmatrix} \tag{2}$$

where Z_{TRS} is the series impedance of the 161/69-kV transformer

Z_{TRD} is the series impedance of the 0.69/69-kV transformer

The node-voltage equation of the study system is then given by

$$\begin{bmatrix} I_A \\ I_B \\ I_C \\ I_{T1} \\ I_{T2} \\ I_{M1} \\ I_{M2} \end{bmatrix} = Y_e \begin{bmatrix} V_A \\ V_B \\ V_C \\ V_{T1} \\ V_{T2} \\ V_{M1} \\ V_{M2} \end{bmatrix} \tag{3}$$

where I_A, I_B, I_C : A, B and C phase of the primary current at 161kV side;

$I_{T1}, I_{T2}, I_{M1}, I_{M2}$: T_1 , T_2 , M_1 and M_2 phase of the secondary current at 69kV side;

V_A, V_B, V_C : A, B and C phase of the primary voltage at 161kV side;

$V_{T1}, V_{T2}, V_{M1}, V_{M2}$: T_1 , T_2 , M_1 and M_2 phase of the secondary voltage at 69kV side;

Y_e : node admittance matrix of the study system .

The node admittance matrix of the study system can be obtained using

$$Y_e(i,j) = \begin{bmatrix} Y(i,j)+y & i=j=4,5 \\ Y(i,j)+y & i=4, j=5, or, i=5, j=4 \\ Y(i,j)+y & i=j=6,7 \\ Y(i,j)-y_M & i=6, j=7, or, i=7, j=6 \\ Y(i,j) & other \end{bmatrix} \tag{4}$$

where $Y(i,j)$: node admittance between *i* node and *j* node;.

y_T : admittance of *T* phase;

y_M : admittance of *M* phase;

It can also be found that

$$\begin{bmatrix} V_A \\ V_B \\ V_C \\ V_{T2} \end{bmatrix} = \begin{bmatrix} V_{SA} - \frac{I_A}{y_{src}} \\ V_{SB} - \frac{I_B}{y_{src}} \\ V_{SC} - \frac{I_C}{y_{src}} \\ V_{T1} - \frac{I_T}{y_T} \end{bmatrix} \text{ and } \begin{bmatrix} V_{M2} \\ I_{T2} \\ I_{M2} \\ V_T \\ V_M \end{bmatrix} = \begin{bmatrix} V_{M1} - \frac{I_M}{y_M} \\ I_{T1} \\ I_M \\ \frac{I_T}{y_T} \\ \frac{I_M}{y_M} \end{bmatrix} \tag{5}$$

where V_{SA}, V_{SB}, V_{SC} : A, B and C phase of the source voltage at 161kV side;

To obtain the current $\begin{bmatrix} I_A & I_B & I_C & I_{T1} & I_{T2} & I_{M1} & I_{M2} \end{bmatrix}^T$ matrix in (3), we first set the initial value for voltage matrix $\begin{bmatrix} V_A & V_B & V_C & V_{T1} & V_{T2} & V_{M1} & V_{M2} \end{bmatrix}^T$; Then, the last voltage matrix was obtained after several iterations. The relation in (5) demonstrates that the (3) can be rearranged as

$$\begin{aligned} f_1(I_A, I_B, I_C, I_T, I_M, V_T, V_M) &= c_1 \\ f_2(I_A, I_B, I_C, I_T, I_M, V_T, V_M) &= c_2 \\ f_3(I_A, I_B, I_C, I_T, I_M, V_T, V_M) &= c_3 \\ f_4(I_A, I_B, I_C, I_T, I_M, V_T, V_M) &= c_4 \\ f_5(I_A, I_B, I_C, I_T, I_M, V_T, V_M) &= c_5 \\ f_6(I_A, I_B, I_C, I_T, I_M, V_T, V_M) &= c_6 \\ f_7(I_A, I_B, I_C, I_T, I_M, V_T, V_M) &= c_7 \end{aligned} \tag{6}$$

In (6) indicate that the seven equations, solving seven unknown parameters.

where $c_1, c_2, c_3, c_4, c_5, c_6$ *and* c_7: constant value of function $f_1, f_2, f_3, f_4, f_5, f_6$ *and* f_7.

The delta-constant value $\Delta C^{(k)}$ at *k* generation of iterative procedures by using Newton's method be described as

$$\Delta C^{(k)} = J^{(k)} \Delta X^{(k)} \tag{7}$$

$$X^{(k+1)} = X^{(k)} + \Delta X^{(k)} \tag{8}$$

Where $\Delta X^{(k)}$ was represent current matrix for A, B, C, T, M phase and T, M phase voltage phase.

$$\Delta X^{(k)} = \begin{bmatrix} \Delta I_A{}^{(k)} \\ \Delta I_B{}^{(k)} \\ \Delta I_C{}^{(k)} \\ \Delta I_T{}^{(k)} \\ \Delta I_M{}^{(k)} \\ \Delta V_T{}^{(k)} \\ \Delta V_M{}^{(k)} \end{bmatrix} \text{ and } \Delta C^{(k)} = \begin{bmatrix} c_1 - (f_1)^{(k)} \\ c_2 - (f_2)^{(k)} \\ c_3 - (f_3)^{(k)} \\ c_4 - (f_4)^{(k)} \\ c_5 - (f_5)^{(k)} \\ c_6 - (f_6)^{(k)} \\ c_7 - (f_7)^{(k)} \end{bmatrix} \tag{9}$$

The Jacobian matrix is

$$J^{(k)} = \begin{bmatrix} (\frac{\partial f_1}{\partial I_A})^{(k)} & (\frac{\partial f_1}{\partial I_B})^{(k)} & (\frac{\partial f_1}{\partial I_C})^{(k)} & (\frac{\partial f_1}{\partial I_T})^{(k)} & (\frac{\partial f_1}{\partial I_M})^{(k)} & (\frac{\partial f_1}{\partial V_T})^{(k)} & (\frac{\partial f_1}{\partial V_M})^{(k)} \\ (\frac{\partial f_2}{\partial I_A})^{(k)} & (\frac{\partial f_2}{\partial I_B})^{(k)} & (\frac{\partial f_2}{\partial I_C})^{(k)} & (\frac{\partial f_2}{\partial I_T})^{(k)} & (\frac{\partial f_2}{\partial I_M})^{(k)} & (\frac{\partial f_2}{\partial V_T})^{(k)} & (\frac{\partial f_2}{\partial V_M})^{(k)} \\ (\frac{\partial f_3}{\partial I_A})^{(k)} & (\frac{\partial f_3}{\partial I_B})^{(k)} & (\frac{\partial f_3}{\partial I_C})^{(k)} & (\frac{\partial f_3}{\partial I_T})^{(k)} & (\frac{\partial f_3}{\partial I_M})^{(k)} & (\frac{\partial f_3}{\partial V_T})^{(k)} & (\frac{\partial f_3}{\partial V_M})^{(k)} \\ (\frac{\partial f_4}{\partial I_A})^{(k)} & (\frac{\partial f_4}{\partial I_B})^{(k)} & (\frac{\partial f_4}{\partial I_C})^{(k)} & (\frac{\partial f_4}{\partial I_T})^{(k)} & (\frac{\partial f_4}{\partial I_M})^{(k)} & (\frac{\partial f_4}{\partial V_T})^{(k)} & (\frac{\partial f_4}{\partial V_M})^{(k)} \\ (\frac{\partial f_5}{\partial I_A})^{(k)} & (\frac{\partial f_5}{\partial I_B})^{(k)} & (\frac{\partial f_5}{\partial I_C})^{(k)} & (\frac{\partial f_5}{\partial I_T})^{(k)} & (\frac{\partial f_5}{\partial I_M})^{(k)} & (\frac{\partial f_5}{\partial V_T})^{(k)} & (\frac{\partial f_5}{\partial V_M})^{(k)} \\ (\frac{\partial f_6}{\partial I_A})^{(k)} & (\frac{\partial f_6}{\partial I_B})^{(k)} & (\frac{\partial f_6}{\partial I_C})^{(k)} & (\frac{\partial f_6}{\partial I_T})^{(k)} & (\frac{\partial f_6}{\partial I_M})^{(k)} & (\frac{\partial f_6}{\partial V_T})^{(k)} & (\frac{\partial f_6}{\partial V_M})^{(k)} \\ (\frac{\partial f_7}{\partial I_A})^{(k)} & (\frac{\partial f_7}{\partial I_B})^{(k)} & (\frac{\partial f_7}{\partial I_C})^{(k)} & (\frac{\partial f_7}{\partial I_T})^{(k)} & (\frac{\partial f_7}{\partial I_M})^{(k)} & (\frac{\partial f_7}{\partial V_T})^{(k)} & (\frac{\partial f_7}{\partial V_M})^{(k)} \end{bmatrix} \tag{10}$$

The system fault types include

(a) Two-phase balanced fault: short circuit faults in both phase T and phase M loads.

There are short circuit faults at the 27.5-kV phase T and phase M loads. Then $Z_{TL} = Z_{ML} = 0$, and $Z_f = 0.1$.

(b) Single-phase unbalanced fault: short circuit fault in phase T or phase M load.

There is a short circuit fault at either the 27.5-kV phase T or phase M load.

(b1) Short circuit fault occurs at phase-T load. Then $Z_{TL}=0$, and $Z_f=0.1$.

(b2) Short circuit fault occurs at phase-M load. Then $Z_{ML}=0$, and $Z_f=0.1$.

Let us take the single-phase unbalanced fault at the phase T load on the 27.5kV side of the power system with the Scott scheme as an example. At the initial stage, let the estimate of the current to be

$$\begin{bmatrix} I_A^{(0)} \\ I_B^{(0)} \\ I_C^{(0)} \\ I_T^{(0)} \\ I_M^{(0)} \\ V_T^{(0)} \\ V_M^{(0)} \end{bmatrix} = \begin{bmatrix} 0 \\ 0 \\ 0 \\ 0 \\ 0 \\ 0 \\ 0 \end{bmatrix} \tag{11}$$

A solution is obtained when the absolute difference between two successive iteration is less than a specified value, i.e.,

$$\left| X^{(k+1)} - X^{(k)} \right| \le \varepsilon \tag{12}$$

where ε is the required accuracy.

At stage k, when the current matrix $\begin{bmatrix} I_A^{(k)} \\ I_B^{(k)} \\ I_C^{(k)} \\ I_T^{(k)} \\ I_M^{(k)} \end{bmatrix}$ is known, the bus voltage matrix $\begin{bmatrix} V_A^{(k)} \\ V_B^{(k)} \\ V_C^{(k)} \\ V_T^{(k)} \\ V_M^{(k)} \end{bmatrix}$ can be obtained by (5).

The current matrix can then be updated using (8). The other equations (7), (9) and (10) are used also. The iteration is repeated until the error between stage *(k+1)* and stage k is acceptable.

2.3 Effect of over-current relay

If the voltage sag is caused by a fault in the DG power system, the duration (Δ t) depends on the fault clearing time during which the protective relay and the circuit breaker (CB) operate. The relay in consideration is the over-current relay (50/51). The operating time of the relay is obtained from the movement curve. The operating time of the circuit breaker is related to the mechanical characteristic and can be regarded as having a constant value. The voltage sag duration can be expressed as

$$\Delta t = t_{Ry} + t_{CB} \tag{13}$$

where t_{Ry} : protective relay operating time.

t_{CB} : circuit breaker operating time.

In a practical distribution system, t_{CB} is between 3 and 8 cycles.

According to the IEC 60255-22 Standard such as IEC Standard 60255-22-2007 (2007), the over current relay (51) inverse t-I curve parameters are given in (14). The α and β values in Table 2 determine the slopes.

$$t_{Ry}(s) = \frac{k\beta}{\left(\frac{I_F}{I_P}\right)^{\alpha} - 1} \tag{14}$$

where k : time multiplier

I_F : fault current detected by relay (normally the effective value).

I_P : current setting threshold.

Table 2 Inverse t-I curve parameter of over-current relay

t-I curve setting		α	β
A	Normal Inverse	0.02	0.14
B	Very Inverse	1.0	13.5
C	Extremely Inverse	2.0	80.0
D	Long-Time Inverse	1.0	120.0

If the normal inverse curve is used, then $\alpha=0.02$, and $\beta=0.14$ can be substituted into (14) to yield the voltage sag duration. The value of $\Delta V_{(F)} \times \Delta t_{(F)}$ can be used to describe the voltage sag range where $\Delta V_{(F)}$ is small change of the drop in voltage, and $\Delta t_{(F)}$ is the duration. From Figure 4, it can be obtained that

$$\Delta V_{(F)} = V_{SFi} - (Z_{TRS} + Z_{TRD}) I_{Fi} \tag{15}$$

where

V_{SFi} is the voltage sag at point *i*

Z_{TRS} is the series impedance of the 161/69-kV transformer

Z_{TRD} is the series impedance of the 0.69/69-kV transformer

I_{Fi} is the fault current at point *i*, $i = A, B, and\, C$. If $I_{Fi} \geq I_p$, then

$$\Delta t_{(F)} = \frac{0.14k}{\left|\frac{I_{Fi}}{I_P}\right|^{0.02} - 1} \quad (16)$$

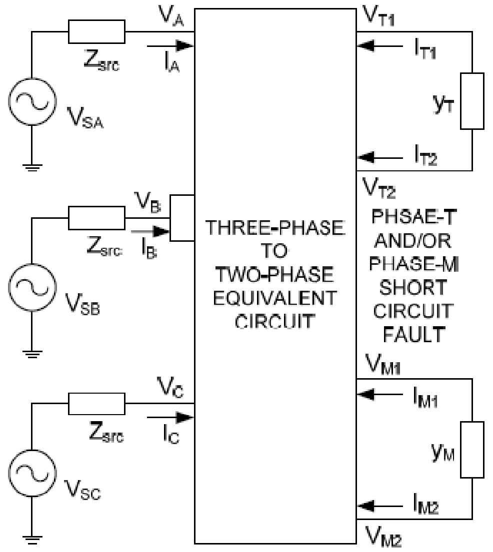

Fig. 4 Short circuit analysis of a power system with specially connected transformers.

2.4 Voltage sag analysis procedure

In this paper, voltage sags analysis is caused by short circuit in the DG power system. In order to determine the voltage at the Interconnected Point of Common Coupling (IPCC) in the DG power system. The model consists of the source impedance Z_S, distributed generation source impedance Z_{DGS}, transformer impedance Z_{TRS}, transmission line impedance Z_{L1}, distributed generation transformer impedance Z_{TRD}, load transformers impedance Z_{TRL}, railway transmission line impedance Z_{L2T}, and Z_{L2M}. All the loads of models are initially supposed to be of the constant impedance type. This allows including the contribution of the loads into the source impedance.

Figure 5 shows a flowchart for the voltage sag calculation. It is described as follows:

(1) Transform system equipment impedances to p.u. values, and input equipment parameters data.

(2) Select equation for fault voltages and currents at all voltage levels are calculated, and the voltage sag ranges $\Delta V_{(F)}$ are obtained.

(3) Choose the curve of the over-current relay (50/51). The relay operating time and the circuit breaker operating time are added to yield the fault clearing time, which is the voltage sag duration $\Delta t_{(F)}$.

(4) Compare $\Delta V_{(F)}$ and $\Delta t_{(F)}$ with the voltage sag acceptability curve (VSAC).

(5) Satisfy the voltage sags of requirement with voltage sag acceptability curve (VSAC).

(6) If the result is not satisfied, PSO is then used to compute the transformer impedance and relay parameter settings.

(7) That is repeated until the voltage sag and duration are acceptable by the change transformer impedance and reset relay parameter.

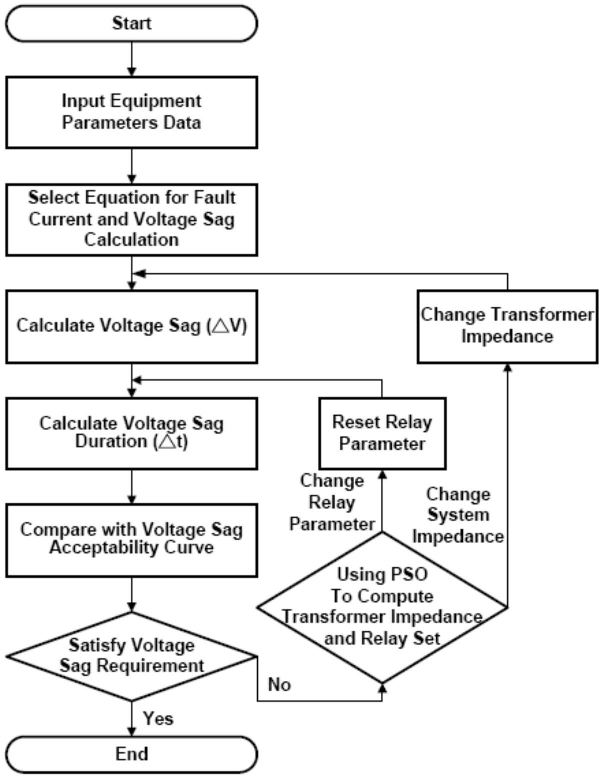

Fig.5 Voltage sag calculation flowchart.

2.5 PSO methods

PSO is originally attributed to Kennedy and Eberhart (1995) first intended for simulating social behavior, as a stylized representation of the movement of organisms in a bird flock or fish school. The algorithm was simplified and observed to perform optimal operation. The book by Kennedy and Eberhart (1995) describes many philosophical aspects of PSO and swarm intelligence.

In computer science, PSO is a computational method that optimizes a problem by iteratively trying to improve a candidate solution with regard to a given measure of quality. PSO optimizes a problem by having a population of candidate solutions, here dubbed particles, and moving these particles around in the search-space according to simple mathematical formula over the particle's position and velocity. Each particle's movement is influenced by its local best known position and is also guided toward the best known positions in the search-space, which are updated as better positions and are found by other particles.

2.6 Problem formulation

The PSO approach is used to obtain the suitable transformer impedances and relay settings. It is described as follows.

2.6.1 Objective function：

Minimize $M = \sqrt{(t_{IPCC\_VSAc} - t_{up})^2 + \rho(V_{IPCC\_VSAc} - V_{up})^2}$ (17)

where t_{IPCC_VSAc}: VSA curve duration time of IPCC;
V_{IPCC_VSAc}: VSA curve voltage of IPCC;
t_{up} : fault duration time of unacceptable point;
V_{up} : fault voltage of unacceptable point;
$\rho = 1$.

and $t_{IPCC\_VSAc} \le t_{up} \cap V_{IPCC\_VSAc} \ge V_{up}$, otherwise M=0

Variable vector: $X = [X_{TRS} \quad X_{TRL} \quad X_{TRD} \quad k]^t$

$$k^{\min} < k < k^{\max}$$

$$X_{TRi}^{min} < X_{TRi} < X_{TRi}^{max} \quad i = S, L, D \tag{18}$$

where k : relay time multiplier;
X_{TRS} , X_{TRL} and X_{TRD} : transformer impedance.

2.6.2 Constraints:

(a) System equipment parameter: The limit conditions of system equipment should be examined.

(b) Voltage regulation: The voltage regulation must be less than 5%. That is

$$-5\% < VR_i < 5\% \qquad i = A, B, C \tag{19}$$

(c) Protective relay coordination: The downstream relay action time must be less than that of the upstream relay. That is,

$$T_{F,27.5kV} < T_{F,69kV} \tag{20}$$

3. Results

Two-phase balanced faults and single-phase unbalanced faults are considered. Figure 4 reveals the simulation system, whose parameters are given in Table 3. The relay follows the normal inverse curve, where α is 0.02 and β is 0.14.

Table 3 System data

Power Source	Balanced three-phase, 161 kV, Y-connected, X/R=33.25, short circuit capacity=10935 MVA
Distributed Generation	Balanced three-phase, 0.69 kV, Y-connected, X/R=33.25, short circuit capacity=40 MVA
Transformer	TRS：3Φ/3Φ, 161/69 kV, 200 MVA, X_{TRS}=13%, X/R=40, △ /Y-g connected, Z_{g1}=20 Ω
	TRD：3Φ/3Φ, 0.69/69 kV, 40 MVA, X_{TRS}=10%, X/R=40, △ /Y-g connected
	TRL：3Φ/2Φ, 69/27.5 kV, 30 MVA, X_{TRL}=10%, X/R=10
Line	Z_{L1}=1.1869+j3.9108 Ω
	Z_{L2T}= Z_{L2M}=0.873+j2.295 Ω
Load	Each of phase T and phase M: 5MW+j3MVAR
Circuit breaker	T_{CB}=0.08 s

3.1. Two-phase balanced fault

Table 4 shows the 69-kV IPCC voltages calculation results when a two-phase balanced fault occurs at the 27.5-kV load bus for the system with the original settings. Figure 6 gives a comparison of the voltage sag values with the VSA curve. It can be found that with the original settings, the voltage sag values at the 69-kV IPCC are below the curve.

Table 4 Calculation results of 69-kV IPCC for a two-phase balanced fault at 27.5-kV load bus of system with original parameter settings (t_{CB}=0.08s)

specially connected transformers	Phase	Fault voltage (pu)	Fault current (pu)	Fault clearing time △t (s)
Scott	Phase-A	0.6933	9.86	0.3714
	Phase-B	0.6768	10.45	
	Phase-C	0.6765	10.33	
Le Blanc	Phase-A	0.6818	10.22	0.3740
	Phase-B	0.6813	10.24	
	Phase-C	0.6813	10.23	

The PSO approach is used to determine suitable transformer impedance and relay k values. Table 5 gives the original settings and limitation conditions. Table 6 shows the 69-kV IPCC calculation results for the system with parameter values determined using the PSO approach. Table 7 gives the parameter values determined using the PSO approach. Table 6 shows the 69-kV IPCC calculation results for the system with parameter values determined using the PSO approach. They are compared with the VSA curve as plotted in Figure 6. When the transformer impedances and relay settings were modified by using the PSO approach, the voltage values were increased and the duration values were decreased in the using system faults.

Table 5 Original settings and limitation conditions

System parameter		Original setting	Limitation
transformer	TRS 3Φ/3Φ 161/69 kV 200 MVA	X_{TRS}=13%	7%≦X_{TRS}≦13%
	TRD 3Φ/3Φ 0.69/69 kV 40 MVA	X_{TRD}=10%	8%≦X_{TRS}≦14%
	TRL 3Φ/2Φ 69/27.5 kV 30 MVA	X_{TRL}=10%	10%≦X_{TRL}≦16%
relay	CO-k	k=0.1	0.01≦k≦0.1

Table 6 Calculation results of 69-kV IPCC for a two-phase balanced fault at 27.5-kV load bus of system with parameter values determined by PSO (t_{CB}=0.08s)

specially connected transformers	Phase	Fault voltage (pu)	Fault current (pu)	Fault clearing time △t (s)
Scott	Phase-A	0.7227	8.98	0.11006
	Phase-B	0.7011	9.74	
	Phase-C	0.7004	9.60	
Le Blanc	Phase-A	0.7009	9.62	0.11018
	Phase-B	0.7004	9.65	
	Phase-C	0.7004	9.64	

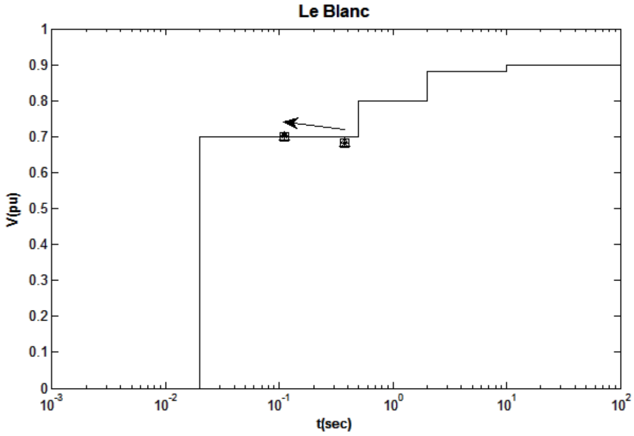

Fig. 6 Comparison of voltage sag values for 69-kV IPCC with VSA curve of the system suffering a two-phase balanced fault at 27.5kV load bus and with parameter settings determined by original and PSO (star：V_A, triangle：V_B, square：V_C).

3.2. Single-phase unbalanced fault

A short circuit fault occurs in phase T at the 27.5-kV load bus, as displayed in Figure 3.To demonstrate the effectiveness of the proposed method, a comparison with PSO, hybrid differential evolution (HDE) and genetic algorithm (GA) for the two-phase fault of Le Blanc scheme is given in Figure 7. It shows the PSO, HDE and GA taking 45, 56 and 128 generations to converge, respectively. The PSO is faster than HDE and GA as shown in Table 7.

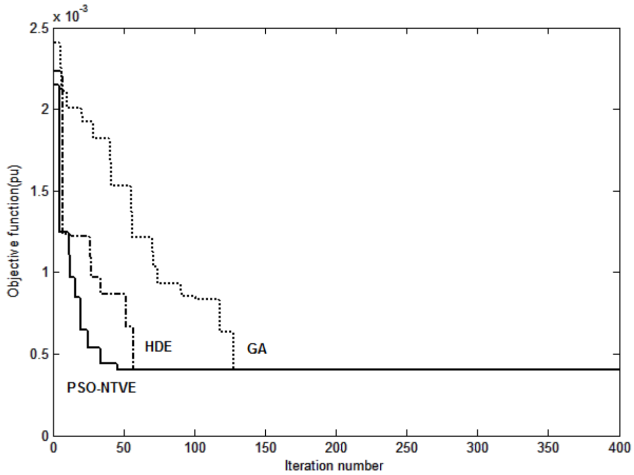

Fig.7 Comparison of convergence characteristics between PSO, HDE and GA for the two-phase fault of Le Blanc scheme

Table 7 Comparison of PSO, HDE and GA for the two-phase fault of Le Blanc scheme

PSO		HDE		GA	
Objective function (p.u.)	0.0004	Objective function (p.u.)	0.0004	Objective function (p.u.)	0.0004
N_P	10	N_P	5	N_P	10
Iteration number	45	Iteration number	56	Iteration number	128
c1	1.5	C_R	0.5	Pc	0.8
c2	1.5	F	0.01	Pm	0.05
		ε1	0.1		
		ε2	0.1		

3.3 Circuit breaker and fault type uncertainty

In previous sections, voltage sags are designed under certain operating conditions. However, since the circuit breaker and fault type operating success fluctuates, practical cases are uncertain. Although the transformer impedance and relay setting parameters were determined, the reliability problems existed in the device manufacturing process and machine aging after installation. Expectation and standard deviation concepts can be used. Table 8 also gives the planning results considering expectation and standard deviation. The proposed method also gives the lowest expectation of the objective function

Table 8 Design results

Specially connected transformers	Phase	Original objective function (p.u.)			PSO objective function (p.u.)			
		two-phase balanced fault	single-phase unbalanced fault (T)	single-phase unbalanced fault (M)	two-phase balanced fault	single-phase unbalanced fault (T)	single-phase unbalanced fault (M)	Expected value (p.u.)
Scott	Phase-A	0.0067	0.0067	0.2915	0.0004	0.0004	0.0004	0.0057
	Phase-B	0.0232	0.2095	0.0832	0.0004	0.0004	0.0004	0.0044
	Phase-C	0.0235	0.2428	0.0438	0.0004	0.0004	0.0004	0.0052
Le Blanc	Phase-A	0.0182	0.0182	0.2915	0.0004	0.0004	0.0004	0.0064
	Phase-B	0.0187	0.2074	0.0900	0.0004	0.0004	0.0004	0.0043
	Phase-C	0.0187	0.2406	0.0503	0.0004	0.0004	0.0004	0.0051

4. Conclusions

In this paper, the influences of two different connection schemes of DG and sensitive loads on the retained voltage during voltage sags in distribution networks are analyzed. The behavior included DG, sensitive loads, and faults generator during voltage sags was verified. This study presented system models of special connection transformers for use in fault analysis. The voltage sag severity of a system with special connection transformers can be controlled by adjusting the transformer impedances and relay settings. Two connection schemes Scott and Le Blanc connection were studied. The node admittance matrix of each scheme was obtained for voltage sag calculation. The optimization approach using the PSO method was used to obtain suitable transformer impedances and relay settings. The results were compared with the VSA curve. The simulation results showed that voltage sag can be improved by using the proposed method. The uncertain condition is also considered using the probability concept in this study.

References

Bollen M. H. J. (1999). *Understanding power quality problems：voltage sags and interruptions*. IEEE Press Series on Power Engineering. New York : The Institute of Electrical and Electronics Engineers.

Chang Y. P. (2010). Integration of SQP and PSO for optimal planning of harmonic filters. *Expert Systems with*

Applications, *37*(1), 2522-2530.

Chen T. H., & Kuo H. Y. (1995). Network modeling of traction substation transformers for studying unbalance effects. *IEE Proceedings-Generation Transmission and Distribution*, 142(2), 103-108.

Deihimi Ali, & Momeni Abolfazl (2012). Neural estimation of voltage-sag waveforms of non-monitored sensitive loads at monitored locations in distribution networks considering DGs. *Electric Power Systems Research*, *92* (1), 123-137.

Das J. C. (1990). Effects of momentary voltage dips on the operation of induction and synchronous motors. *IEEE Transactions on Industry Applications, 26*(4), 711-718.

Gomez J. C., & Morcos M. M. (2002). Voltage sag and recovery time in repetitive events. *IEEE Transactions on Power Delivery*, *17*(4),1037-1043.

He Na, Xu Dianguo, & Huang Lina (2009). The application of particle swarm optimization to passive and hybrid active power filter design. *IEEE Transactions on Industrial Electronics*, *56*(8), 2841- 2851.

Heydt G. T. & Jewell W. T.. Pitfalls of electric power quality indices (1998). *IEEE Transactions on Power Delivery,* 13(2), 570-578.

Huang Sy Ruen, Kuo Yueh Lung, Chan Bing Nan, Lu Kwang Chang, & Huang Min Chiuan (2001). A short circuit current study for the power supply system of Taiwan railway. *IEEE Transactions on Power Delivery*, *16*(4), 492-497.

IEEE Recommended Practice for Emergency and Standby Power Systems for Industrial and commercial Applications (1995). IEEE Standard 446-1995, New York: The Institute of Electrical and Electronics Engineers.

IEEE Recommended Practice for Powering and Grounding Electronic Equipment (2006). IEEE Standard 1100-2005, New York : The Institute of Electrical and Electronics Engineers.

IEEE Recommended Practice for Monitoring Electric Power Quality (1995). IEEE Standard 1159-1995, New York : The Institute of Electrical and Electronics Engineers.

IEEE Standard for Interconnecting Distributed Resources with Electric Power Systems (2008). IEEE Std. 1547™-2008.

IEC Recommended Practice for Single Input Energizing Quality Measuring Relay with Dependent or Independent Time (2007). IEC Standard 60255-22.

Ko C. N., Chang Y. P., & Wu C. J. (2009). A PSO method with nonlinear time-varying evolution for optimal design of harmonic filters. *IEEE Transactions on Power Systems*, 24 (1), 437-444.

Kumar G. Siva, Kalyan Kumar B., & Mishra Mahesh K. (2011). Mitigation of voltage sags with phase jumps by UPQC with PSO-Based ANFIS. *IEEE Transactions on Power Delivery*, 26(4), 2761-2773.

Kyei J., Ayanar R., Heydt G., & Thallam R. (2001). The design of power acceptability curves. *IEEE Transactions on Power Delivery, 17*(3), 828-833.

Kennedy J., & Eberhart R. (1995). *Particle swarm optimization*. Paper presented in the IEEE International Conference on Neural Networks, Perth, Australia.

Lee G. J., Albu M. M., & Heydt G. T. (2004). A power quality index based on equipment sensitivity, cost, and network vulnerability. *IEEE Transactions on Power Delivery*; 19(3), 1504-1510.

Mahdianpoor F. Mohammad, Hooshmand Rahmat Allah, & Ataei Mohammad (2011). A new approach to multifunctional dynamic voltage restorer implementation for emergency control in distribution systems. *IEEE Transactions on Power Delivery*, 26 (2), 882-890.

Macke K. J. P., Bollen M. H. J., & Belmans R. J. M (2004). Mitigation of voltage dips through distributed generation systems. *IEEE Transactions on Industrial Application, 40*(6),1686-1693.

Milanovic J. V., Ali H., & Aung M. T. (2007). Influence of distribution wind generation and load composition on voltage sags, *Inst. Eng. Technol., Gen. Transm. Distrib*. *1*(1), 13-22.

Wang J., Chen S., & Lie T. T.. System voltage sag performance estimation (2005). *IEEE Transactions on Power Delivery, 20*(2), 1738-1747.

Yalcinkaya G., Bollen M. H. J., & Crossley P. A. (1998). Characterization of voltage sags in industrial distribution systems. *IEEE Transactions on Industry Applications,* 34 (4) 682-688.

粒子群最佳化演算法求解含特殊變壓器連接並考量敏感性負載之分散式發電機電壓驟降最佳規劃

張英彬 [1]、楊烈岱 [2]

[1] 南開科技大學 電機與資訊技術系

[2] 南開科技大學 工業管理系

摘　要

本文係探討含分散式發電機系統之三相對兩相轉換史考特與 Le Blanc 兩種特殊變壓器連接電壓驟降最佳規劃。採用粒子群最佳化演算法來決定設計最佳值，同時分析考量敏感性負載與過電流電驛的協調性。文中以節點導納矩陣來組成數學模型，並以單相與兩相故障系統來測試電壓驟降嚴重性。本文首先以分析方程式做爲最佳規劃的數學方法，然後，運用粒子群最佳化演算法，有效獲得合適的變壓器阻抗和電驛時間倍數的參數。爲證實有效測試所提方法有效性與搜尋全域最佳解可能性，本文分別以含有史考特與 Le Blanc 兩種特殊變壓器連接系統進行測試。最後，由研究結果顯示，電壓驟降嚴重性可藉由調整變壓器的阻抗和電驛設定來改善。

關鍵詞：分散式發電機、電壓驟降、電力品質、敏感性負載、粒子群最佳化演算法、特殊變壓器連接